JOURNAL OF VIROLOGY, Apr. 2003, p. 4169–4180 Vol. 77, No. 7
0022-538X/03/$08.00+0 DOI: 10.1128/JVI.77.7.4169–4180.2003

nef Gene Is Required for Robust Productive Infection by Simian Immunodeficiency Virus of T-Cell-Rich Paracortex in Lymph Nodes

Chie Sugimoto,[1] Kei Tadakuma,[1] Isao Otani,[2] Takashi Moritoyo,[3] Hirofumi Akari,[1] Fumiko Ono,[4] Yasuhiro Yoshikawa,[5] Tetsutaro Sata,[6] Shuji Izumo,[3] and Kazuyasu Mori[1,7]*

Tsukuba Primate Center for Medical Sciences, National Institute of Infectious Diseases,[1] and Corporation for Production and Research of Laboratory Primates,[4] Tsukuba 305-0843, Department of Veterinary Medicine, College of Bioresource Sciences, Nihon University, Fujisawa 252-8510,[2] Center for Chronic Viral Disease, Faculty of Medicine, Kagoshima University, Kagoshima 890-0075,[3] Department of Biomedical Science, Faculty of Agriculture, University of Tokyo, Tokyo 113-8657,[5] and AIDS Research Center[7] and Department of Pathology,[6] National Institute of Infectious Diseases, Tokyo 162-8640, Japan

Received 30 September 2002/Accepted 19 December 2002

The pathogenesis of AIDS virus infection in a nonhuman primate AIDS model was studied by comparing plasma viral loads, CD4$^+$ T-cell subpopulations in peripheral blood mononuclear cells, and simian immunodeficiency virus (SIV) infection in lymph nodes for rhesus macaques infected with a pathogenic molecularly cloned SIVmac239 strain and those infected with its *nef* deletion mutant (Δnef). In agreement with many reports, whereas SIVmac239 infection induced AIDS and depletion of memory CD4$^+$ T cells in 2 to 3 years postinfection (p.i.), Δnef infection did not induce any manifestation associated with AIDS up to 6.5 years p.i. To explore the difference in SIV infection in lymphoid tissues, we biopsied lymph nodes at 2, 8, 72, and 82 weeks p.i. and analyzed them by pathological techniques. Maximal numbers of SIV-infected cells (SIV Gag$^+$, Env$^+$, and RNA$^+$) were detected at 2 weeks p.i. in both the SIVmac239-infected animals and the Δnef-infected animals. In the SIVmac239-infected animals, most of the infected cells were localized in the T-cell-rich paracortex, whereas in the Δnef-infected animals, most were localized in B-cell-rich follicles and in the border region between the paracortex and the follicles. Analyses by double staining of CD68$^+$ macrophages and SIV Gag$^+$ cells and by double staining of CD3$^+$ T cells and SIV Env$^+$ cells revealed that SIV-infected cells were identified as CD4$^+$ T cells in either the SIVmac239 or the Δnef infection. Whereas the many functions of Nef protein were reported from in vitro studies, our finding of SIVmac239 replication in the T-cell-rich paracortex in the lymph nodes supports the reported roles of Nef protein in T-cell activation and enhancement of viral infectivity. Furthermore, the abundance of SIVmac239 infection and the paucity of Δnef infection in the T-cell-rich paracortex accounted for the differences in viral replication and pathogenicity between SIVmac239 and the Δnef mutant. Thus, our in vivo study indicated that the *nef* gene enhances SIV replication by robust productive infection in memory CD4$^+$ T cells in the T-cell-rich region in lymphoid tissues.

The importance of the *nef* gene of simian immunodeficiency virus (SIV) for persistent active viral replication has been demonstrated in a macaque AIDS model (26). Defects in the *nef* gene not only lowered the magnitude of SIV infection but also allowed the host immune system to induce protective immunity against pathogenic SIVs (12, 24, 25). Findings of defective *nef* alleles in human immunodeficiency virus (HIV) isolates from infected individuals who have been categorized as long-term nonprogressors were the driving force behind studies on protective immunity against the AIDS virus (28). Based on those studies, the *nef* gene is generally accepted to play a key role in the pathogenesis of HIV/SIV (primate AIDS virus) infection (13). The functions of the *nef* gene in primate AIDS virus replication in vitro or ex vivo have been reported; they include enhancement of viral infectivity (20, 33), mediation of T-cell activation (4, 15, 32, 48), and down-regulation of cell surface molecules such as CD4 (1, 18), major histocompatibility complex (MHC) class I (21, 30), and CD28 in CD4$^+$ T cells (52). However, the functions of the *nef* gene in the primate AIDS virus in vivo still remain unclear (for reviews, see references 17, 25, and 41).

The importance of early events in AIDS virus infection in terms of viral replication, host immune response, and disease progression has been reported from HIV type 1 (HIV-1) clinical studies (45) and studies of animal AIDS models (34). In particular, due to considerations of feasibility in study design, early events of SIV infection in macaques were extensively investigated by examination of various tissues, viral strains, and infection routes (9, 10, 23, 29, 39, 44, 50, 51, 54–57). Reimann et al., using SIVmac251, reported that SIV-infected cells localized predominantly in T-cell-rich extrafollicular regions in lymph nodes (LNs) at primary infection (44). Lackner et al. performed extensive analyses of the spleen and thymus and reported similar results for SIVmac239 infection. They also found that cells infected with an attenuated strain, SIVmac1A11, were localized in follicles (29). The results of Chakrabarti et al. with SIVmac251 were relatively consistent with those of Reimann et al. and Lackner et al., but they also noted SIV$^+$ cells scattered in the cortex (corresponding to follicles) at day 4 postinfection (p.i.) (9). Chakrabarti et al. found productive infection by a SIVmac251 *nef* mutant in

* Corresponding author. Mailing address: Tsukuba Primate Center for Medical Science, National Institute of Infectious Diseases, 1 Hachimandai, Tsukuba 305-0843, Japan. Phone: 81-298-37-2121. Fax: 81-298-37-0218. E-mail: mori@nih.go.jp.

TABLE 1. Antibodies used in immunohistochemistry study

Antibody name (clone)	Stained cell type	Source[a]	Antigen retrieval method[b]
SIV Gag (rabbit polyclonal)	SIV-infected cell	T. Sata	Pronase
SIV Env gp160/gp32 (KK41)	SIV-infected cell	K. Kent	0.1 M citrate buffer (pH 7.0) plus autoclave
SIV Nef aa 71–80	SIV-infected cell	FIT Biotech	0.1 M citrate buffer (pH 6.0) plus autoclave
CD3 (rabbit polyclonal)	T cell	Dako	Pronase or 0.1 M citrate buffer (pH 7.0) plus autoclave[c]
CD4 (1F6)	$CD4^+$ T cell	Novocastra	0.1 M citrate buffer (pH 6.0) plus autoclave
CD68 (KP1)	Macrophage	Dako	Pronase
CD20 (L26)	B cell	Dako	Pronase
PCNA (PC10)	Proliferating cell	Dako	0.1 M citrate buffer (pH 6.0) plus autoclave
TIA-1 (2G9A10F5)	CTL, NK	Beckman Coulter	0.1 M citrate buffer (pH 7.0) plus autoclave

[a] T. Sata, National Institute of Infectious Diseases, Tokyo, Japan; K. Kent, NIBSC, Hertfordshire, United Kingdom; FIT Biotech, Tampere, Finland; Novocastra, Newcastle, United Kingdom; Beckman Coulter, Tokyo, Japan.
[b] Collected tissues were fixed with paraformaldehyde and then embedded in paraffin.
[c] Sections were treated with pronase for single staining or with 0.1 M citrate buffer (pH 7.0) and autoclaving for double staining with an anti-Env antibody, KK41.

germinal centers (GC) at day 7 p.i. and subsequent trapping of SIV virions in GC at day 15 p.i. (10). Stahl-Henning et al. examined localization of SIV-infected cells in tonsils at day 4 p.i. for macaques infected with SIVmac251 by an oral mucosal route (50); they found that whereas SIV-infected cells were observed in all compartments of the tonsils, the majority were $CD4^+$ T cells in extrafollicular lymphoid tissue equivalent to the paracortex in LNs. Taken together, the results from these five studies show that pathogenic SIVmac251 and SIVmac239 infection occurred in both the T-cell-rich paracortex and follicles and that Δ*nef* mutants and an attenuated strain, SIVmac1A11, replicated in follicles in LNs. Thus, early events after SIV infection are assumed to determine the outcome of AIDS virus infection, that is, whether the infected host controls the infection or not. Furthermore, we assumed that the *nef* gene plays an important role in determining these early events after primate AIDS virus infection.

In this study, to clarify the role of the *nef* gene in SIV replication in vivo, we infected rhesus macaques with a molecularly cloned SIVmac239 with a functional *nef* gene as a wild-type virus or with its *nef* deletion mutant (Δnef). SIVmac239 infection induced AIDS in two of the three animals by 3 years p.i., and Δnef mutant infection was suppressed to low viral loads without any manifestation associated with AIDS except a gradual decline in naïve CD4 T cells. We examined SIV infection in the LNs at weeks 2, 8, 72, and 82 p.i. At the peak of the primary infection, SIV-infected cells were observed in different locations in the LNs: for the SIVmac239-infected animals, most of the infected cells were localized in the T-cell-rich paracortex, whereas for the Δnef-infected animals, most were localized in B-cell-rich follicles. Our in vivo study indicated that the *nef* gene enhances SIV replication by robust productive infection in memory $CD4^+$ T cells in the T-cell-rich paracortex in lymphoid tissues.

MATERIALS AND METHODS

Viruses. Proviral DNAs of wild-type SIVmac239 *nef*$^+$ (SIVmac239) and a mutant with a 183-bp deletion in the *nef* gene (Δnef) were provided by Ronald C. Desrosiers (New England Regional Primate Research Center, Harvard Medical School, Southborough, Mass.) (26). Stocks of SIVmac239 and Δnef were produced by DNA transfection of the respective infectious DNAs into COS1 cells (34, 35). For SIV infection of monkeys, these virus stocks were propagated in phytohemagglutinin (PHA)-stimulated peripheral blood mononuclear cells (PBMCs) from rhesus macaques, and their titers (50% tissue culture infective doses [$TCID_{50}$]) were determined on CEMx174 cells (34, 35).

Animal infection studies. Eight juvenile rhesus macaques of Burmese or Laotian origin that were seronegative for SIV, simian T-lymphotropic virus, B virus, and type D retroviruses were used. All animals were housed in individual cages and maintained according to the National Institute of Infectious Diseases rules and guidelines for experimental animal welfare. Animals were infected intravenously with 100 $TCID_{50}$ of SIVmac239 (animals Mm18, Mm24, Mm27, Mm06, and Mm22) or Δnef (animals Mm14, Mm16, and Mm29).

Determination of plasma viral loads by real time PCR. SIV infection was monitored by measuring the plasma viral load. Viral RNA was isolated from plasma from infected animals by using a commercial viral RNA isolation kit (Roche Diagnostics, Tokyo, Japan). SIV *gag* RNA was amplified and quantified by using a commercial RNA reverse transcription-PCR kit (TaqMan EZ RT-PCR; Perkin-Elmer Applied Biosystems, Urayasu, Japan) with two *gag* primers, namely, the forward primer 1224F (5′-AATGCAGAGCCCCAAGAAGAC-3′) and the reverse primer 1326R (5′-GGACCAAGGCCTAAAAAACCC-3′), and with the TaqMan probe 1272T (FAM-5′-ACCATGTTATGGCCAAATGCCC AGAC-3′-TAMRA). Purified viral RNA (10 μl) was reverse transcribed and amplified in a MicroAmp optical 96-well reaction plate (Perkin-Elmer Applied Biosystems) according to the manufacturer's instructions and with the following thermal cycle conditions: 1 cycle of three sequential incubations (50°C for 2 min, 60°C for 30 min, and 95°C for 5 min), followed by 50 cycles of amplification (95°C for 5 s and 62°C for 30 s) in a 7700 prism sequence detection system (Perkin-Elmer Applied Biosystems). In vitro RNA transcripts were quantified by measurement of optical density at 260 nm and a branched-DNA assay for SIV viral RNA (Bayer Diagnostics, Tarrytown, N.Y). RNA equivalent to 10 to 10^7 copies per reaction was used as a standard for each assay. The detection sensitivity of plasma viral RNA by this method was 10^3 copies/ml.

Flow cytometry. CD4 depletion was monitored by measuring the absolute number (or count) of $CD4^+$ T cells in the blood and the percentages of memory and naïve $CD4^+$ T cells in PBMCs. PBMC samples were purified from citrate-anticoagulant-containing blood by standard Ficoll-Hypaque gradient centrifugation. For flow cytometry, 2×10^5 PBMCs were reacted with fluorescein isothiocyanate (FITC)- or phycoerythrin (PE)-labeled antibodies (anti-human CD4 antibody Nu-Th/I [Nichirei, Tokyo, Japan], anti-human CD8 antibody Leu2a [Becton Dickinson, San Jose, Calif.], anti-human CD29 antibody 4B4 [Coulter, Miami, Fla.], anti-monkey CD3 antibody FN-18 [Biosource, Camarillo, Calif.], and anti-human CD20 antibody Leu16 [Becton Dickinson]) as previously described (2). PBMC counts in blood samples were determined by using an automated blood cell counter (Sysmex, Kobe, Japan). Absolute CD4 counts were calculated by multiplying the PBMC count in blood by the percentage of $CD4^+$ T cells.

Tissue collection. In the first experiment, biopsies of inguinal or axillary LNs of all six infected monkeys (Mm18, Mm24, and Mm27 infected with SIVmac239; Mm14, Mm16, and Mm29 infected with the Δnef mutant) were carried out at 2, 8, and 72 weeks p.i. (for Mm14, Mm16, Mm29, and Mm27) or 82 weeks p.i. (for Mm18 and Mm24). In the second experiment, two rhesus macaques (Mm06 and Mm22) infected with SIVmac239 were biopsied at days 4 and 7 p.i. and autopsied at day 11 p.i. (Mm06) or day 14 p.i. (Mm22). Collected LNs were fixed with 4% paraformaldehyde for 24 h and then embedded in paraffin. For routine histopathological examination, tissues were stained with hematoxylin-eosin.

Immunohistochemistry. We analyzed the phenotypes of the cells by immunohistochemical methods with fluorescein or regular 3,3′-diamidebenzidine (DAB) as a chromogen. Detailed information on the antibodies used in this study is

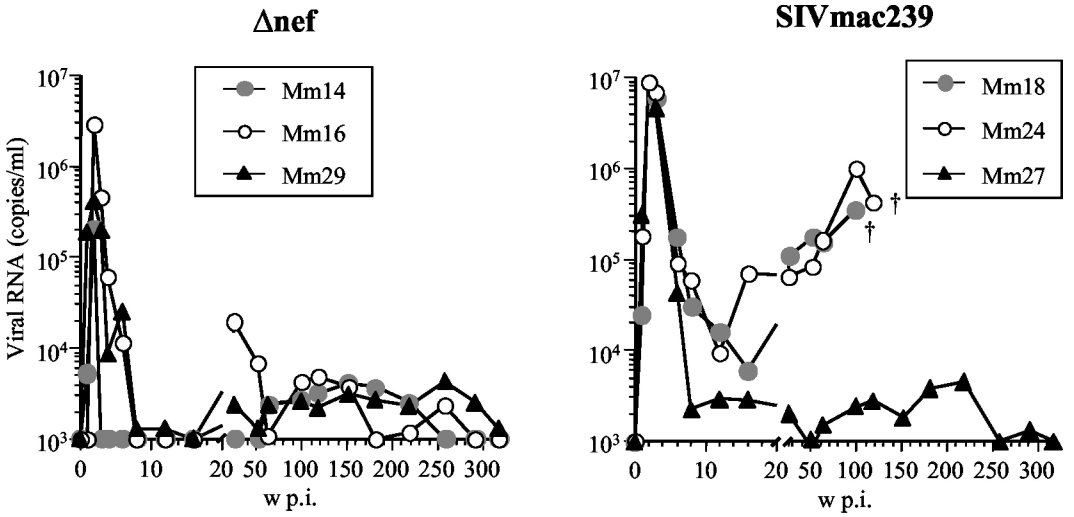

FIG. 1. Replication of SIVmac239 and Δnef in rhesus macaques based on plasma viral RNA load after intravenous inoculation with 100 $TCID_{50}$ of the respective virus. †, animals Mm18 and Mm24 died of AIDS at 106 and 133 weeks (w) p.i., respectively.

given in Table 1. Paraffin-treated sections were dewaxed and pretreated by appropriate methods for each antibody (Table 1).

For double staining (combination of anti-p27 Gag and anti-CD68, anti-p27 Gag and anti-CD35, or anti-Env gp160/gp32 and anti-CD3), sections were incubated with both primary antibodies either at 4°C overnight or at 37°C for 1 h. After a wash with Tris-buffered saline and blocking with TNB (0.1 M Tris-HCl [pH 7.5]–0.15 M NaCl–0.5% blocking reagent), sections were incubated at room temperature for 1 h with Envision+ rabbit, a peroxidase-labeled anti-rabbit immunoglobulin (Ig) polymer (Dako, Kyoto, Japan), for the rabbit polyclonal antibody and with a biotin-conjugated anti-mouse IgG (Dako) for monoclonal antibodies. After a wash, the immobilized peroxidase-labeled Ig on the sections was visualized with fluorescein tyramide by using a Tyramide Signal Amplification (TSA) kit (Perkin-Elmer Life Science, Boston, Mass.). Subsequently, sections were incubated with Alexa 594-conjugated streptavidin (Molecular Probes, Eugene, Oreg.) for visualization of immobilized biotin-conjugated IgG.

For single staining (anti-SIV Env gp160/gp32, anti-SIV Nef, anti-CD4, anti-CD20, anti-CD3, TIA1, and PCNA), sections were incubated first with the primary antibody and then with Envision+ rabbit or mouse (Dako) as the secondary antibody. Sections were visualized by TSA or a metal-enhanced DAB substrate (Pierce, Rockford, Ill.).

Finally, sections were mounted with VECTASHIELD mounting medium and 4′,6′-diamidino-2-phenylindole (DAPI) (Vector Laboratories, Burlingame, Calif.) for immunofluorescein staining or with MOUNT QUICK for DAB staining. Sections were examined with a fluorescence microscope system (BX50 + BX-FLA; Olympus, Tokyo, Japan) equipped with a digital camera (DP50) and a personal computer.

To examine the location specificity of SIV replication in LNs, SIV protein-containing (Gag^+ or Env^+) cells in the paracortex, B-cell-rich follicles, and border region (region containing scattered B cells) were counted by using the serial sections stained with antibodies against SIV proteins and with an anti-CD20 antibody.

In situ hybridization. For in situ hybridization, we used riboprobes that were complementary to SIV *gag*, *pol*, and *nef* regions and were labeled by incorporation of digoxigenin-UTP (Roche Diagnostics). SIV RNA was detected in tissue sections by in situ hybridization as previously described (36, 39). Briefly, dewaxed sections were pretreated with 0.2 N hydrochloric acid for 20 min, digested with 20 μg of proteinase K/ml at 37°C for 15 min, and acetylated. For hybridization, 2 μg of SIV probe mixture/ml in 50% deionized formamide–10% dextran sulfate–600 mM NaCl–10 mM Tris (pH 7.5)–1 mM EDTA–200 μg of yeast RNA/ml–0.25% sodium dodecyl sulfate–1× Denhardt's solution was annealed at 50°C overnight in a humid chamber. After a wash in 2× SSC (1× SSC is 0.15 M NaCl plus 0.015 M sodium citrate) at 55°C for 1 h and another in 0.2× SSC at 50°C for 40 min, the sections were incubated with a sheep anti-digoxigenin antibody conjugated with alkaline phosphatase (Roche Diagnostics). Bound probes were finally visualized with the alkaline phosphatase substrate nitroblue tetrazolium (NBT)–5-bromo-4-chloro-3-indolylphosphate (BCIP) in the substrate buffer. Sections were counterstained with Kernechtrot solution.

RESULTS

Plasma viral loads in rhesus macaques infected with either SIVmac239 or Δnef. Three rhesus macaques were intravenously infected with 100 $TCID_{50}$ of SIVmac239 with a functional *nef* gene (SIVmac239), and three were infected with a mutant virus with a 183-bp deletion in the *nef* gene (Δnef). Two patterns of infection were seen in the three rhesus macaques infected with SIVmac239 (Fig. 1). During the first 4 weeks p.i., SIV replicated synchronously in all three animals; a peak in the primary infection was seen at 2 weeks p.i. for all three (2×10^7, 9×10^6, and 1.3×10^7 SIV RNA copies/ml for Mm18, Mm24, and Mm27, respectively). However, the set points and viral loads diverged into two paths thereafter. Incomplete suppression of primary infection with a set point of 10^4 copies/ml was seen for two of the three animals (Mm18 and Mm24). For these two animals, viral loads continued to increase to the end points; Mm18 died of AIDS at 106 weeks p.i., and Mm24 was euthanized due to AIDS symptoms at 133 weeks p.i. In contrast, for the other animal (Mm27), SIV infection was suppressed after the primary infection with a set point below 10^3 copies/ml, and even in the chronic phase, the viral load remained on the order of 10^3 copies/ml up to 330 weeks p.i. (Fig. 1).

For the three rhesus macaques infected with Δnef, primary infections occurred with kinetics similar to those observed for the monkeys with the SIVmac239 infection, as described in the preceding paragraph. Peak viral loads were detected for all three animals (2×10^5, 3×10^6, and 4×10^5 copies/ml for Mm14, Mm16, and Mm29, respectively) at 2 weeks p.i. Despite the differences in the peak viral loads among the three animals, each viral load decreased sharply to below the detection sensitivity (10^3 copies/ml) by 8 weeks p.i. In the chronic phase, viral loads remained below 10^4 copies/ml in all three animals (Fig. 1).

$CD29^{high}$ and $CD29^{low}$ subpopulations in $CD4^+$ T cells. Subpopulations of $CD4^+$ $CD29^{high}$ T cells and $CD4^+$ $CD29^{low}$ T cells, which are closely related to memory and naïve $CD4^+$ T cells, respectively, have been used to monitor disease pro-

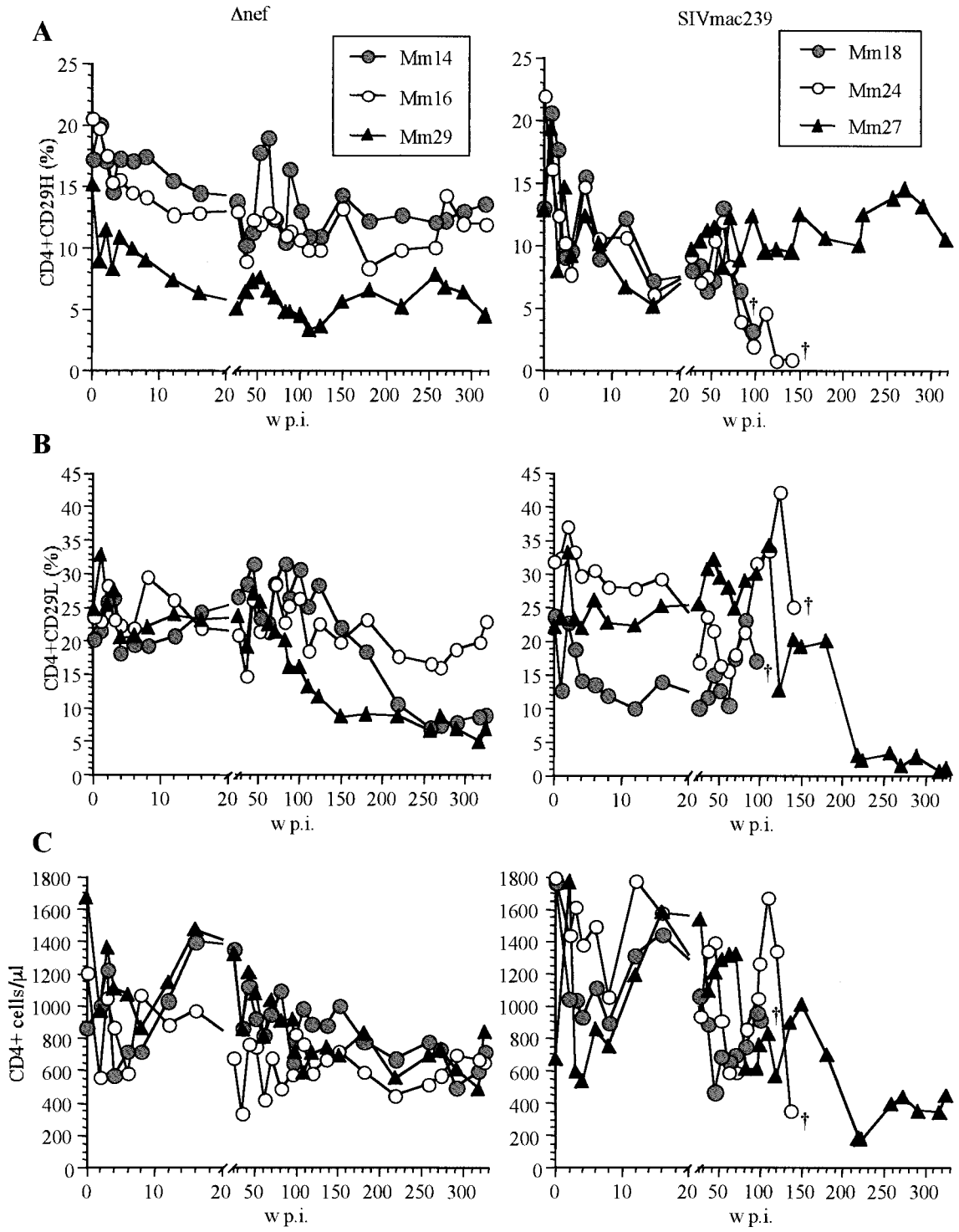

FIG. 2. $CD4^+$ T cells in rhesus macaques infected with Δnef or SIVmac239. (A) Percentage of $CD4^+$ $CD29^{high}$ T cells in PBMCs; (B) percentage of $CD4^+$ $CD29^{low}$ T cells in PBMCs; (C) absolute $CD4^+$ T-cell counts in blood.

gression in HIV-infected individuals and in an SIV AIDS animal model (8, 31, 37). Therefore, we monitored these $CD4^+$ T-cell subpopulations in SIV-infected animals. In the two animals that developed AIDS (Mm18 and Mm24), the $CD4^+$ $CD29^{high}$ subpopulation dropped below 5% after 80 weeks p.i. By contrast, in the other four animals, which maintained low viral loads for more than 6 years, the $CD4^+$ $CD29^{high}$ subpopulation remained at preinfection levels (Fig. 2A). Thus, longitudinal changes in the levels of $CD4^+$ $CD29^{high}$ T cells in PBMCs correlated well with disease progression in SIVmac239-infected animals (Fig. 2A).

In contrast to the $CD4^+$ $CD29^{high}$ subpopulation, less-dras-

tic decreases in the $CD4^+$ $CD29^{low}$ subpopulation were detected at the time of autopsy or euthanasia for the two animals that developed AIDS (Mm18 and Mm24). In addition, this subpopulation ($CD4^+$ $CD29^{low}$) decreased gradually after 1.5 years p.i. in three of the four animals (Mm27, Mm14, and Mm29) that maintained low viral loads for more than 6 years (Fig. 2B). Only for one animal (Mm16) did both $CD29^{high}$ and $CD29^{low}$ $CD4^+$ T-cell subpopulations remain at preinfection levels for more than 6 years.

Because of the distinct kinetics of $CD29^{high}$ and $CD29^{low}$ populations, blood $CD4^+$ T-cell counts did not correlate with pathogenic development and viral load for the SIVmac239-infected animals. Only one animal (Mm24) exhibited a sharp drop in $CD4^+$ T-cell counts, partly due to lymphocytopenia, at the time of euthanasia at 133 weeks p.i., although the CD4 count had increased at 109 weeks p.i. (Fig. 2C). Another disease progressor (Mm18) also showed an increase in the CD4 count near the time of death at 99 weeks p.i.

The CD29 marker does not accurately define memory and naïve $CD4^+$ T cells: whereas $CD4^+$ $CD29^{low}$ T cells correspond to naïve $CD4^+$ T cells, $CD4^+$ $CD29^{high}$ T cells contain both memory and naïve $CD4^+$ T cells (42; L. J. Picker, personal communication). Nevertheless, these results indicated that different extents of SIV replication in the chronic phase influenced different CD4 subpopulations in PBMCs: whereas high SIV replication was associated with depletion of memory $CD4^+$ T cells, long-term low-level SIV infection was associated with a decline in naïve $CD4^+$ T cells.

Histology and $CD4^+$ cell depletion in surface LNs from SIVmac239- and Δnef-infected animals. AIDS virus infection is well known to occur predominantly in $CD4^+$ T cells and macrophages in lymphatic tissue in vivo. Therefore, we examined the histology and distribution of $CD4^+$ cells and SIV infection in biopsied surface LNs. Activated GC were observed at 2 weeks p.i. in LNs from Δnef-infected animals (Fig. 3A), and moderately activated follicles were observed in those from SIVmac239-infected animals (Fig. 3B); however, this histological difference was reversed at chronic infection (72 or 82 weeks p.i.). Whereas only a small GC was observed in Δnef-infected animals, many large GC were observed in SIVmac239-infected animals (Fig. 3C and D). Consistent with plasma viral loads, many SIV Gag^+ cells were detected in LNs taken at 2 weeks p.i. from Δnef-infected animals (Fig. 3E) and SIVmac239-infected animals (Fig. 3F). SIV Gag^+ cells localized differently in LNs in the two infected groups. Many SIV^+ cells were inside and around the GC in Δnef-infected animals (Fig. 3A and E), whereas most of the SIV-infected cells were outside the follicles in SIVmac239-infected animals (Fig. 3B and F). As the viral load decreased at 72 weeks p.i. (Fig. 1), few SIV^+ cells were detected in Δnef-infected animals (Fig. 3G). In SIVmac239-infected animals with high viral loads (Mm24 [Fig. 1]), SIV^+ signals were densely accumulated in GC in LNs taken at 82 weeks p.i. (Fig. 3H). These signals were found to be SIV virions trapped on follicular dendritic cells (FDC), because of the nature of diffused Gag^+ signals and the overlap with $CD35^+$ (a C3b receptor which is an FDC marker) signals (Fig. 3I, J, and M). In addition, CD4 cell depletion was also evident in LNs from SIVmac239-infected animals (Fig. 3L) but not in LNs from Δnef-infected animals (Fig. 3K).

Δnef-infected cells preferentially localized in follicles of LNs at primary infection. Using serial sections from LNs biopsied at 2 weeks p.i., we stained SIV RNA^+ cells by in situ hybridization and stained B cells with an anti-CD20 antibody by immunohistochemistry. SIV RNA^+ cells were localized inside B-cell-rich follicles in Δnef-infected animals but were localized in the paracortex in SIVmac239-infected animals (Fig. 4). Furthermore, we examined multiple sections from multiple LNs from each of the six animals by immunohistochemistry with antibodies against SIV proteins (Fig. 5). For both groups of infected animals, the most distinct localization was seen in sections with many SIV^+ cells (Table 2). However, in both groups, some SIV-infected cells were in border regions between the follicles and the paracortex (Fig. 5; Table 2). We estimated the proportions of SIV-infected cells in the paracortex, B-cell-rich follicles, and border region in LNs at 2 weeks p.i. for each of the six animals (Table 2). Eighty percent of the SIV^+ cells were localized in the T-cell-rich paracortex in SIVmac239-infected animals, whereas less than 10% of the SIV^+ cells were detected in the same region, and the majority of the remaining cells were in B-cell-rich follicles or the border region, in Δnef-infected animals. Because the frequency of SIV^+ cells in SIVmac239-infected animals was higher than that in Δnef-infected animals, we concluded that the difference in localization of SIV^+ cells could be explained by the paucity of SIV replication in the paracortices of Δnef-infected animals.

The majority of SIV^+ cells were $CD68^-$ $CD3^+$ cells in both Δnef-infected and SIVmac239-infected animals. $CD4^+$ T cells and macrophages are the major cell types in rhesus macaques infected with pathogenic SIVs (9, 10, 23, 29, 50, 54, 55). We therefore examined if the differential localization of infected cells is due to localization of target cells in LNs at 2 weeks p.i. Using an anti-CD68 monoclonal antibody and an anti-SIV Gag p27 rabbit antibody, we did double staining of SIV^+ cells and $CD68^+$ macrophages. As shown in Fig. 6, SIV^+ cells (green) and macrophages (red) did not overlap in LNs from either Δnef-infected or SIVmac239-infected animals (Fig. 6A, E, I, and M). Using serial sections, we stained $CD4^+$ T cells to examine the cell type of SIV^+ cells (Fig. 6B and J). Because many $CD4^+$ cells coexisted with SIV^+ cells, most of the SIV^+ cells in both SIVmac239-infected and Δnef-infected animals were likely $CD4^+$ T cells. Next, we did double staining of SIV Env^+ cells (red) and $CD3^+$ T cells (green) by using an anti-SIV Env mouse monoclonal antibody and an anti-CD3 rabbit antibody. Most SIV Env^+ cells overlapped with $CD3^+$ cells (Fig. 6F, G, H, N, O, and P). Thus, SIV productively infected $CD4^+$ T cells in LNs in both Δnef-infected and SIVmac239-infected animals.

Using another serial section, we stained $CD20^+$ B cells to define B-cell-rich follicles and the paracortex (Fig. 6C and K). The location of SIV^+ cells in LNs was confirmed. We also stained for TIA1, a marker of effector cells (cytotoxic T lymphocytes [CTL] or natural killer [NK] cells). Whereas many $TIA1^+$ cells localized proximal to SIV-infected cells in the paracortex of a SIVmac239-infected animal, apparently fewer $TIA1^+$ cells localized in the B-cell-rich follicles of a Δnef-infected animal (Fig. 6D and L).

SIV-infected cells in LNs at day 7 p.i. At 2 weeks p.i, the peak of primary infection, SIV-infected cells localized differentially depending on the function of the *nef* gene. SIVmac239-infected cells predominantly localized in the T-cell-rich para-

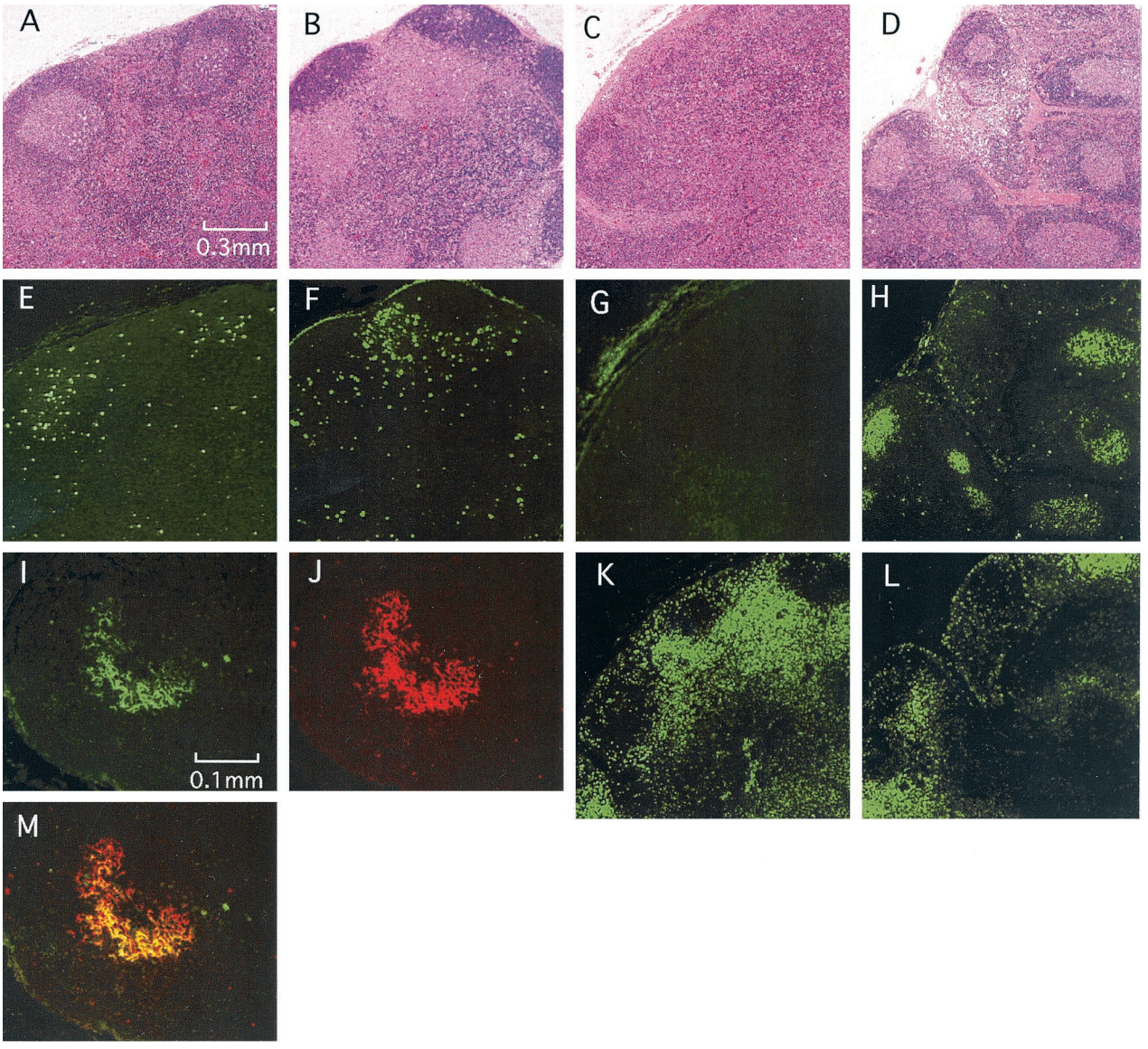

FIG. 3. Histology and immunohistochemical staining of LN samples taken at 2 weeks p.i. and at 72 or 82 weeks p.i. from a rhesus macaque (Mm16) infected with Δnef or from rhesus macaques (Mm18 and Mm24) infected with SIVmac239. (A through D) Hematoxylin-eosin staining of LN sections from Mm16 at 2 weeks p.i. (A), Mm18 at 2 weeks p.i. (B), Mm16 at 72 weeks p.i. (C), and Mm24 at 82 weeks p.i. (D). (E through H) Immunostaining of SIV p27 Gag protein in sections from Mm16 at 2 weeks p.i. (E), Mm18 at 2 weeks p.i. (F), Mm16 at 72 weeks p.i. (G), and Mm24 at 82 weeks p.i. (H). (I, J, and M) Immunostaining of FDC network in GC of Mm24 at 82 weeks p.i. (I) SIV p27 Gag; (J)CD35$^+$ cells (FDC); (M) double staining of SIV p27 Gag and CD35. (K and L) Immunostaining of CD4$^+$ cells from Mm16 at 72 weeks p.i. (K) and Mm24 at 82 weeks p.i. (L). The following combinations of panels represent staining of serial sections: A and E; B and F; C, G, and K; and D, H, and L.

cortex. One question arises: does this distinctive localization of SIV productive infection occur only at the peak of the primary infection? SIV infection might move into an LN depending on the susceptibility of the target cells to SIV replication. For example, the initial infection takes place in the most susceptible cells, fully activated CD4$^+$ T cells, and then infection spreads to resting memory CD4$^+$ T cells. To examine this hypothesis, we biopsied LNs from two SIVmac239-infected animals at days 4 and 7 p.i. and examined the SIV infection. In LNs from autopsies at days 11 and 14 p.i., SIV Env$^+$ cells were predominantly detected in the paracortex, as with the three animals infected with SIVmac239 in the first experiment (Mm18, Mm24, and Mm27). At day 4 p.i., no SIV Env$^+$ cells were detected by fluorescent-staining immunohistochemistry. At day 7 p.i., the earliest time at which SIV Env$^+$ cells were detected, 60 to 70% of productively infected cells were localized in the border region between B-cell-rich follicles and the T-cell-rich paracortex (Fig. 7; Table 2). These results indicate that T cells in the border region were highly susceptible to SIV infection in LNs. These results also suggest that SIVmac239 infection then spread to many T cells in the paracortex, whereas Δnef infection spread to T cells in the B-cell-rich follicles.

Development of GC and anti-SIV antibody titer. As described in the preceding section, we observed larger GC in LNs

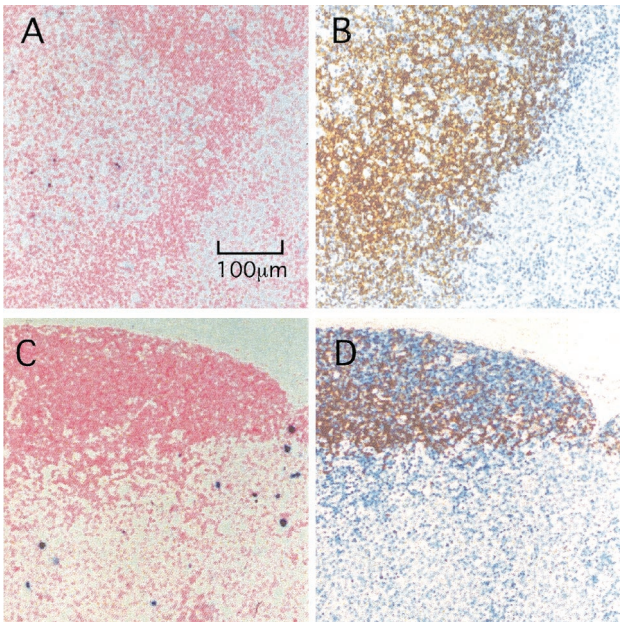

FIG. 4. SIV RNA$^+$ cells in LN samples taken at 2 weeks p.i. from a Δnef-infected (Mm16) and a SIVmac239-infected (Mm18) rhesus macaque. (A and B) Mm16; (C and D) Mm18. Serially sectioned tissue specimens were stained either by in situ hybridization with antisense SIVmac239 RNA (A and C) or with an anti-CD20 antibody (B and D) to stain B cells. SIV RNA$^+$ cells (blue) were localized in a region rich in CD20$^+$ B cells (brown) in LNs of rhesus macaques infected with Δnef. By contrast, SIV RNA$^+$ cells were localized outside a region rich in CD20$^+$ B cells in LNs of rhesus macaques infected with SIVmac239.

in the Δnef infection than in the SIVmac239 infection (Fig. 3A and B). To see the difference in the development of the B-cell-rich follicles in the two groups, we stained CD20$^+$ cells and PCNA (a marker of proliferating cells)-positive cells in LN specimens taken at 2 weeks p.i. from SIVmac239- and Δnef-infected animals. Greater numbers of GC and B-cell-rich follicles were observed for Δnef-infected animals than for SIVmac239-infected animals (Fig. 8).

To examine whether the difference in GC formation influenced the development of an anti-SIV humoral response in SIV-infected animals, we assayed anti-SIV enzyme-linked immunosorbent assay (ELISA) titers for SIVmac239- and Δnef-infected animals. We detected anti-SIV IgG 1 week earlier in the animals with SIVmac239 infection (at 3 weeks p.i.) than in those with Δnef infection (Fig. 9). As expected from the difference in plasma viral loads, anti-SIV antibody titers in SIVmac239-infected animals were higher than those in Δnef-infected animals throughout the infection (Fig. 9). Collectively we observed more-extensive development of GC in Δnef infection than in SIVmac239 infection. However, the difference in GC development did not correlate with the difference in the anti-SIV IgG antibody response between SIVmac239 infection and Δnef infection.

DISCUSSION

Because we compared infections with wild-type SIVmac239 and its Δnef mutant in LNs, the paucity of SIV infection in the T-cell-rich paracortex must have been due to a defect in the *nef*

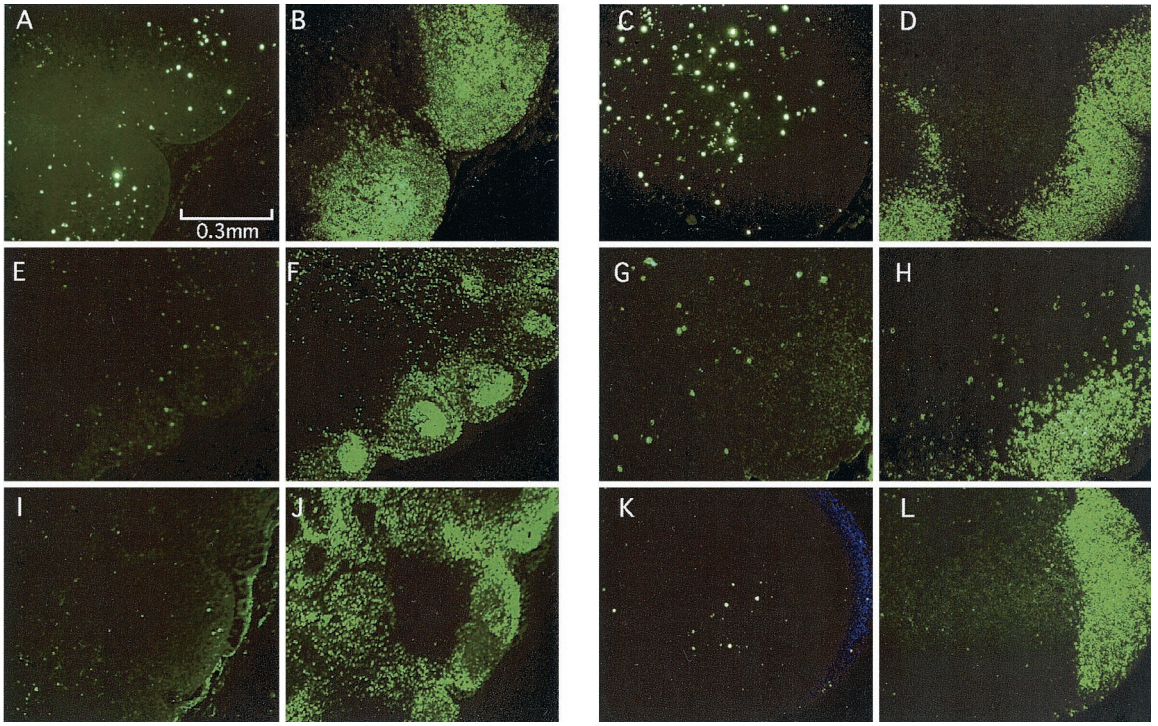

FIG. 5. SIV Env$^+$ cells in LNs at 2 weeks p.i. Serially sectioned tissue specimens were stained either with an anti-SIV gp32 Env antibody (A, C, E, G, I, and K) or with an anti-CD20 antibody (B, D, F, H, J, and L) to stain B cells. (Left panels) LNs of rhesus macaques infected with Δnef: Mm16 (A and B), Mm14 (E and F), and Mm29 (I and J). (Right panels) LNs of rhesus macaques infected with SIVmac239: Mm18 (C and D), Mm24 (G and H), and Mm27 (K and L).

TABLE 2. Localization of SIV$^+$ cells in LNs

Expt and virus	Animal	Time of biopsy[a]	No. (%) of SIV$^+$ cells in:			Frequency of SIV$^+$ cells (no./mm^2)
			Paracortex	Border[b]	Follicles[c]	
Expt 1						
SIVmac239	Mm18	2 wk	202 (84.9)	22 (9.2)	14 (5.9)	79.3
	Mm24	2 wk	74 (77.9)	17 (17.9)	4 (4.2)	16.1
	Mm27	2 wk	81 (85.3)	10 (10.5)	4 (4.2)	19.8
Δnef	Mm14	2 wk	1 (6.7)	8 (53.3)	6 (40)	4.7
	Mm16	2 wk	9 (7.4)	21 (17.2)	92 (75.4)	23.9
	Mm29	2 wk	0 (0)	5 (50)	5 (50)	2.6
Expt 2, SIVmac239	Mm06	7 days	1 (10)	7 (70)	2 (20)	1.7
	Mm22	7 days	5 (21.7)	14 (60.9)	4 (17.4)	4

[a] No. of days or weeks p.i.
[b] Region proximal to follicles or containing scattered B cells.
[c] Region containing densely accumulated B cells.

gene. Thus, Nef protein did play an important role in facilitating SIV replication in CD4$^+$ T cells in the paracortex. Conversely, why did the Δnef mutant preferentially infect CD4$^+$ T cells in B-cell-rich follicles rather than in the paracortex, despite the fact that there are more CD4$^+$ T cells in the paracortex? The answer is probably related to the requirement of CD4$^+$ T-cell properties for productive infection by primate AIDS virus. HIV preferentially replicates in memory CD4$^+$ T cells in vitro (47, 49). For SIV-infected animals, depletion of memory CD4 T cells during the primary infection in gut lymphoid tissues (54, 55) and PBMCs (3) has been reported. Because of the predominant use of CCR5 as a viral receptor for SIV infection, CCR5 expression is another requirement for productive SIV infection in vivo (56). From these reports, CCR5$^+$ memory CD4$^+$ T cells are the major target cells for SIV infection in vivo. Then, for productive infection by Δnef, what is the subpopulation of CD4$^+$ T cells that resides in B-cell-rich follicles but not in the paracortex? This subpopulation is likely the activated helper CD4$^+$ T cells that have migrated to GC from the paracortex. CD4$^+$ T cells in GC reportedly are major cells involved in HIV replication in early infection (53). In a human tonsil study, CD57$^+$ CXCR5$^+$ T cells were localized only in GC (and thus are referred to as GC helper T cells) and expressed the surface markers CD45RO (memory marker) and CD69 (early activation marker) (27). Therefore, such CD4$^+$ T cells might be the major target cells for Δnef as well as the initial targets for SIVmac239.

The next question is what cells are productively infected with SIVmac239 but not with Δnef at the peak of primary infection (2 weeks p.i.). We considered a well-described *nef* function, activation of resting memory CD4$^+$ T cells. From an immunological viewpoint, secondary lymphatic tissues, such as LNs and spleen, contain central memory T cells that localize in the T-cell-rich paracortex (46). Because highly activated memory CD4$^+$ T cells are the initial targets of SIV infection in vivo (55), the resting memory CD4$^+$ T cells in the paracortex might subsequently be productively infected by SIVmac239 after the cells are fully activated with the help of the Nef protein.

In vitro studies on Nef function indicated that Nef enhances viral replication by increasing infectivity (33). The findings of Miller et al. (33) and of a study on replication of HIV-1 strain NL4-3 and its Δnef mutant in human tonsil lymphoid histoculture (20) were mostly consistent with the results of our study. Thus, the difference in SIV infection in LNs might be due to the difference in the infectivities of SIVmac239 and Δnef for the resting memory CD4$^+$ T cells in the paracortex. Furthermore, replication of HIV-1 strain NL4-3 but not of its Δnef mutant was efficiently enhanced by addition of interleukin-2 to the culture. Thus, this study appeared to support a role for Nef in T-cell activation, suggesting a common in vivo function of the Nef proteins of HIV-1 and SIVmac239.

Other *nef* functions also might account for SIV replication in the T-cell-rich paracortex. These infected cells might evade an anti-SIV immune response by CTL via MHC class I (MHC-I) down-modulation, which is caused by Nef protein in infected cells (for a review, see reference 13). Relevant to this function, we observed higher numbers of TIA1$^+$ effector (CTL or NK) cells in the paracortex in than in the follicles at 2 weeks p.i. in both SIVmac239 infection and Δnef infection (Fig. 6D and L; also data not shown). Therefore, the difference in the number of SIV-infected cells in the paracortex may be due to MHC-I down-regulation in SIVmac239 infection. Munch et al. reported that Nef-mediated MHC-I down-modulation provided a selective advantage for viral replication in SIVmac239 *nef* mutant-infected macaques (37). However, in vivo studies on MHC-I down-regulation by Nef were controversial. Patel et al. reported that Nef-mediated regulation of MHC-I expression does not appear to be critical for the increased replicative ability of pathogenic SIVmne variants (40). Furthermore, the emergence of CTL escape mutants during primary infection also raised questions on the role of MHC-I down-regulation for immune evasion against CTL (38). Thus, the relevance of Nef function for MHC-I down-regulation in vivo still remains to be elucidated.

In the spread of SIV infection, the initial target cells might be the activated helper CD4$^+$ T cells, as mentioned. Garside et al. visualized migration and interaction of antigen-specific T cells and B cells in LNs (19), revealing that T cells were initially activated in the T-cell-rich paracortex and then migrated to the border region between the paracortex and the follicles, where specific T cells and B cells interacted through binding of CD40 ligand (CD40L) in T cells to CD40 on B cells. In our study, the earliest detected SIV-infected cells were at the border region at day 7 p.i. in SIVmac239 infection (Fig. 7). Many SIV-in-

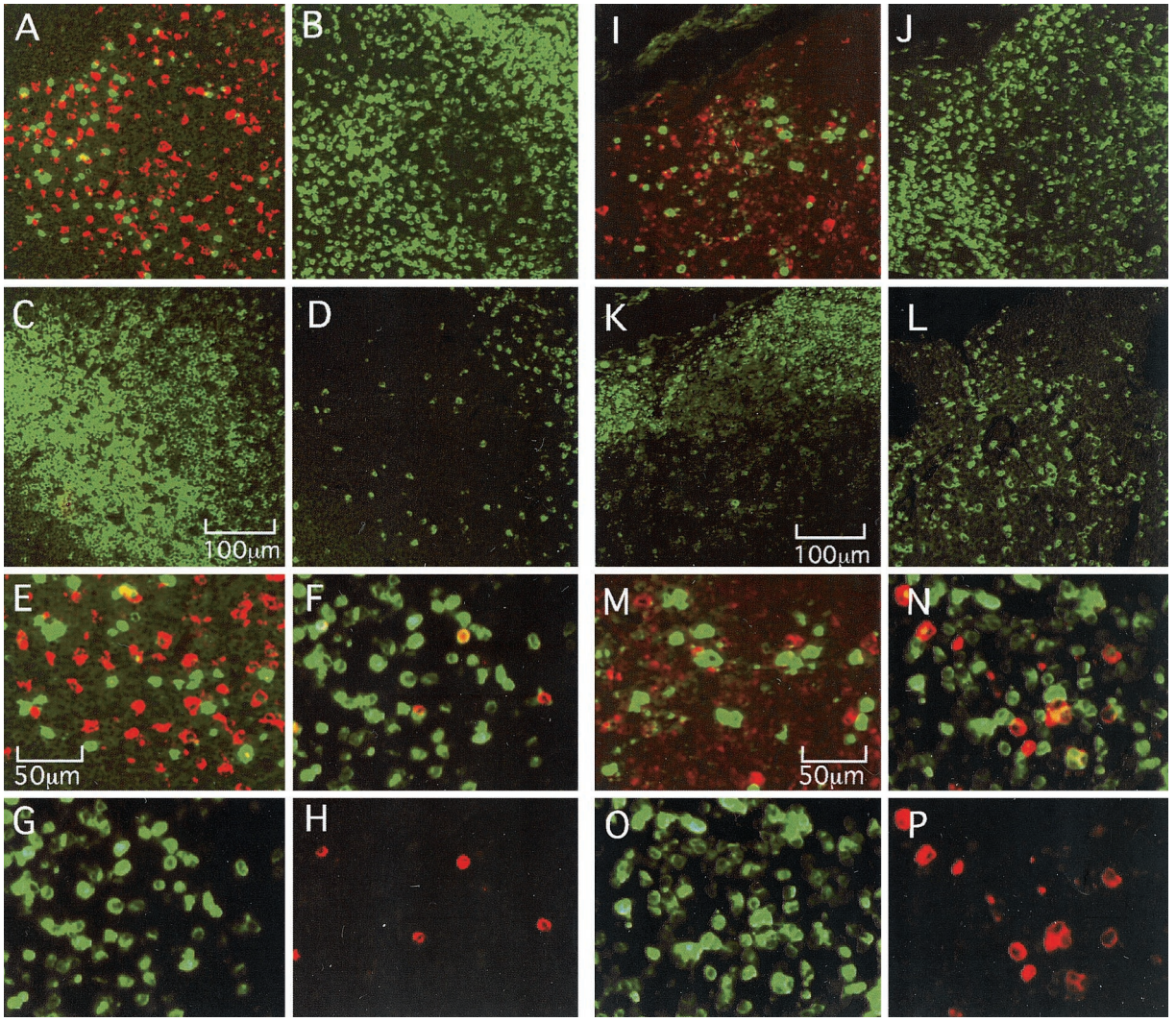

FIG. 6. Identification of SIV$^+$ cells in LN samples taken from the Δnef-infected rhesus macaque Mm16 (A through H) and the SIVmac239-infected rhesus macaque Mm18 (I through P) at 2 weeks p.i. (A, E, I, and M) Double staining with an anti-SIV p27 Gag antibody (green) and an anti-CD68 (macrophage marker) monoclonal antibody (red). Panels E and M are enlarged photos of panels A and I. (B and J) Staining with an anti-CD4 antibody; (C and K) staining with an anti-CD20 (B-cell marker) antibody; (D and L) staining with an anti-TIA1 (CTL and NK marker) antibody; (F and N) double staining with an anti-SIV Env gp160/gp32 monoclonal antibody (red) and an anti-CD3 (T-cell marker) antibody (green); (G and O) staining with the anti-CD3 antibody (green) alone; (H and P) staining with the anti-SIV Env antibody (red) alone. The following combinations of panels represent staining of serial sections: A, B, C, and D; I, J, K, and L.

fected cells were also located in nearly the same regions in the Δnef-infected animals at 2 weeks p.i. (Fig. 5 and Table 2). Therefore, SIV infection may influence the helper T-cell function required for the proper immune response. Poudrier et al. observed impaired CD40L expression in CD4$^+$ T cells and discussed the association with impaired helper T-cell functions in HIV-1 transgenic mice. They reported similar impairment of GC formation in transgenic mice that harbored HIV-1 with a functional *nef* gene but not with a mutated *nef* allele (43). They also demonstrated the impairment of Ig isotype switching from IgM to IgG in the transgenic mice. Relevant to these results, SIV-infected macaques that succumbed rapidly to AIDS often lacked a SIV-specific IgG antibody (16). However, an anti-SIV IgG response occurred in slow disease progressors, as we observed in SIVmac239-infected animals (Mm18 and Mm24)

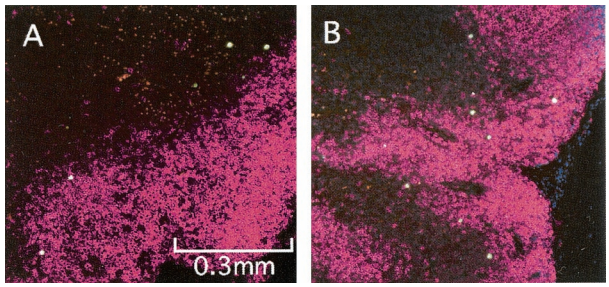

FIG. 7. SIV Env$^+$ cells in LN biopsy samples taken at day 7 p.i. from rhesus macaques infected with SIVmac239. Serially sectioned tissue specimens were stained with either an anti-SIV Env gp160/gp32 antibody or an anti-CD20 antibody. The color of anti-CD20 antibody staining was digitally changed and combined with the image of anti-SIV Env antibody staining. The combined images indicate that SIV Env$^+$ cells (green) were in the border region between the paracortex and B-cell-rich follicles (red). (A) Mm06; (B) Mm22.

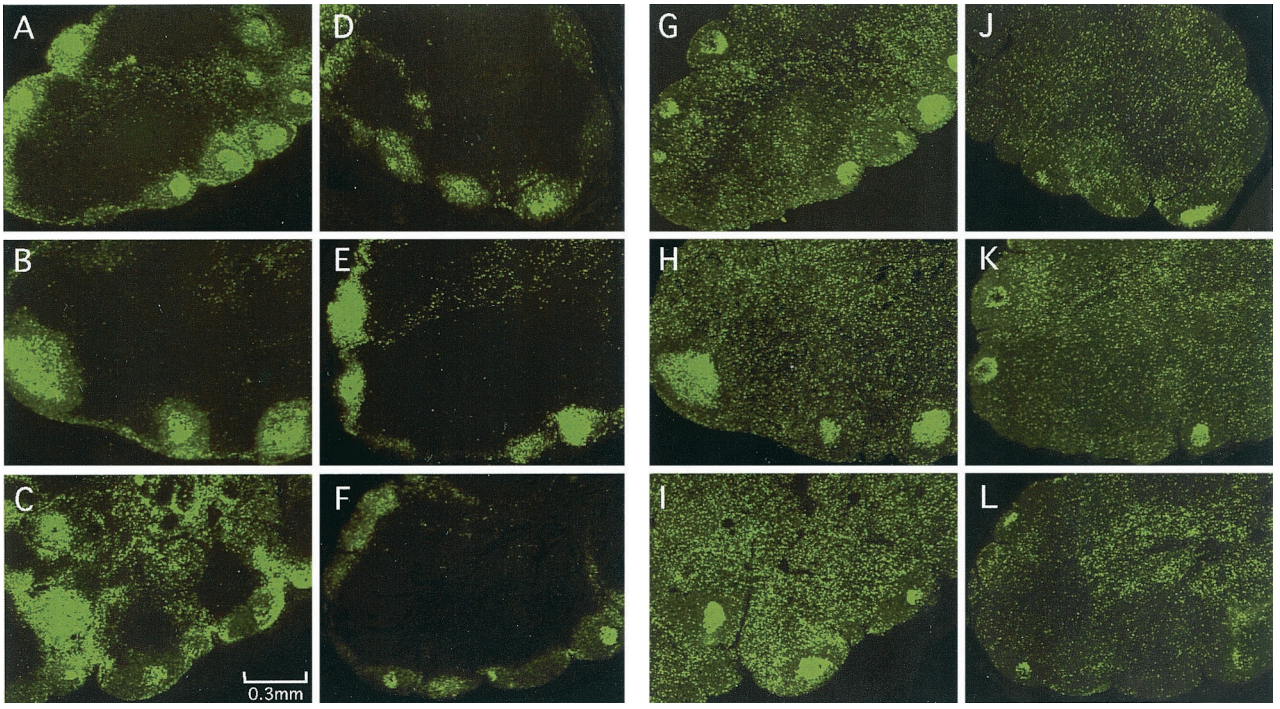

FIG. 8. GC of LNs at 2 weeks p.i. Serial sections of LNs were stained with an anti-CD20 antibody (A through F) or an anti-PCNA (proliferating-cell marker) antibody (G through L) to visualize the GC. (A and G) Mm14; (B and H) Mm16; (C and I) Mm29; (D and J) Mm18; (E and K) Mm24; (F and L) Mm27.

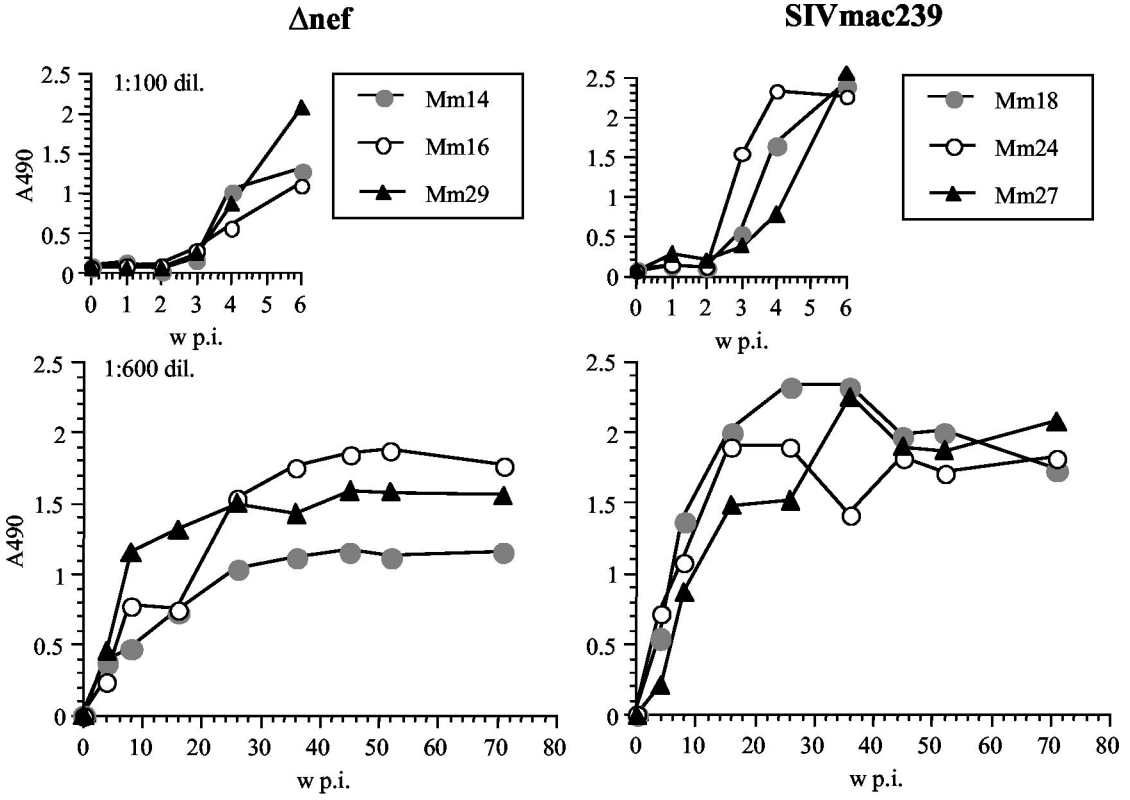

FIG. 9. Anti-SIV ELISA. The optical density at 490 nm was used as a relative measure of antibody titer. Shown are results for 1:100-diluted (top left) and 1:600-diluted (bottom left) plasma from Δnef-infected animals and for 1:100-diluted (top right) and 1:600-diluted (bottom right) plasma from SIVmac239-infected animals. w, weeks.

(16) (Fig. 9). Thus, the extent of impairment of helper T-cell function may determine the disease course in SIV/HIV infection. Fewer and smaller GC in SIVmac239 infection than in Δnef infection might imply a delay in the development of the humoral response, but this delay might be compensated for by strong antigen stimulation due to vigorous viral replication in SIVmac239 infection (Fig. 9). Indeed, we observed similar extensive development of GC in both groups at 8 weeks p.i. (data not shown).

After the primary infection, a SIV-specific immune response suppressed viral infection in both groups, as seen by viral load results (Fig. 1). However, the difference in viral replication in the T-cell-rich paracortex led to different paths of viral replication and host immune response for the two groups: the Δnef mutant infected fewer memory $CD4^+$ T cells in the paracortex, and therefore helper T-cell functions might have been impaired to a lesser extent than in SIVmac239 infection. In fact, high numbers of SIV-specific $CD8^+$ T cells and $CD4^+$ T cells were maintained in the Δnef mutant infection (C. Sugimoto and K. Mori, unpublished data). Therefore, these SIV-specific cellular immune responses might play an important role in control of SIV infection in the chronic phase (Fig. 1). In contrast, presumably due to destruction of SIV-specific $CD4^+$ T cells as reported for HIV-1 infection (14), SIV-specific $CD8^+$ T cells were depleted in SIVmac239-infected animals (Sugimoto and Mori, unpublished). As SIV-specific cellular responses decreased, a second increase in viral replication resulted in AIDS in two of the three animals infected with SIVmac239 (Fig. 1). Hence, the extent of SIV replication in the T-cell-rich regions in lymphatic tissue during primary infection might determine the pathogenic outcome of SIV infection.

Δnef mutants of SIV have been used as prototype viruses for attenuated vaccine virus and have been found to induce protective immunity against pathogenic SIVs (12, 24). However, the pathogenic potential of SIV attenuated vaccine strains was reported for newborn macaques and adult macaques (6, 7). Our results provide evidence of the pathogenic potential of a Δnef mutant for juvenile macaques. Relatively high viral loads were noted in Δnef-infected animals compared with those in animals infected with other attenuated SIVs (11, 24). Our results also revealed a gradual decline in the naïve $CD4^+$ T-cell population in two of the three animals (Mm14 and Mm29), despite a stable presence of the memory $CD4^+$ T-cell population (Fig. 2A and B). Because depletion of naïve $CD4^+$ T cells occurs during HIV infection (22), these two animals need to be monitored for the development of AIDS-related symptoms.

Animals infected with attenuated SIVs in testing for vaccine development exhibit nearly sterilizing immunity against pathogenic SIVs (12, 24, 34). On the other hand, safer vaccine regimens, such as DNA priming and modified vaccinia virus Ankara boosting, successfully controlled chronic infection but failed to control primary infection, thus allowing dissemination of SIV-infected cells throughout the body (5). Therefore, further study is needed to elucidate the mechanisms of nearly sterilizing immunity and of the underlying pathogenicity in attenuated-SIV infection in order to develop a safe vaccine.

ACKNOWLEDGMENTS

We thank Ronald C. Desrosiers and Andrew A. Lackner for reviewing the manuscript before submission. We also thank Karen Kent for providing the monoclonal antibody to SIV gp160/gp32 through the EU Programme EVA/MRC Centralised Facility for AIDS Reagents, NIBSC, United Kingdom (grants QLK2-CT-1999-00609 and GP828102).

This work was supported by AIDS research grants from the Health Sciences Research Grants, from the Ministry of Health, Labour, and Welfare of Japan, and from the Ministry of Education, Culture, Sports, Science and Technology of Japan.

REFERENCES

1. **Aiken, C., J. Konner, N. R. Landau, M. E. Lenburg, and D. Trono.** 1994. Nef induces CD4 endocytosis: requirement for a critical dileucine motif in the membrane-proximal CD4 cytoplasmic domain. Cell **76:**853–864.
2. **Akari, H., K. Mori, I. Otani, K. Terao, F. Ono, A. Adachi, and Y. Yoshikawa.** 1998. Induction of MHC-IIDR expression on circulating $CD8^+$ lymphocytes in macaques infected with SIVmac239 nef-open but not with its nef-deletion mutant. AIDS Res. Hum. Retrovir. **14:**619–625.
3. **Akari, H., K. H. Nam, K. Mori, I. Otani, H. Shibata, A. Adachi, K. Terao, and Y. Yoshikawa.** 1999. Effects of SIVmac infection on peripheral blood $CD4^+$ $CD8^+$ T lymphocytes in cynomolgus macaques. Clin. Immunol. **91:** 321–329.
4. **Alexander, L., Z. Du, M. Rosenzweig, J. U. Jung, and R. C. Desrosiers.** 1997. A role for natural simian immunodeficiency virus and human immunodeficiency virus type 1 *nef* alleles in lymphocyte activation. J. Virol. **71:**6094–6099.
5. **Amara, R. R., F. Villinger, J. D. Altman, S. L. Lydy, S. P. O'Neil, S. I. Staprans, D. C. Montefiori, Y. Xu, J. G. Herndon, L. S. Wyatt, M. A. Candido, N. L. Kozyr, P. L. Earl, J. M. Smith, H.-L. Ma, B. D. Grimm, M. L. Hulsey, J. Miller, H. M. McClure, J. M. McNicholl, B. Moss, and H. L. Robinson.** 2001. Control of mucosal challenge and prevention of AIDS by a multiprotein DNA/MVA vaccine. Science **292:**69–74.
6. **Baba, T. W., A. M. Trichel, L. An, V. Liska, L. N. Martin, M. Murphey-Corb, and R. M. Ruprecht.** 1996. Infection and AIDS in adult macaques after nontraumatic oral exposure to cell-free SIV. Science **272:**1486–1489.
7. **Baba, T. W., V. Liska, A. H. Khimani, N. B. Ray, P. J. Dailey, D. Penninck, R. Bronson, M. F. Greene, H. M. McClure, L. N. Martin, and R. M. Ruprecht.** 1999. Live attenuated, multiply deleted simian immunodeficiency virus causes AIDS in infant and adult macaques. Nat. Med. **5:**194–203.
8. **Blatt, S. P., W. F. McCarthy, B. Bucko-Krasnicka, G. P. Melcher, R. N. Boswell, J. Dolan, T. M. Freeman, J. M. Rusnak, R. E. Hensley, W. W. Ward, D. Barnes, and C. W. Hendrix.** 1995. Multivariate models for predicting progression to AIDS and survival in human immunodeficiency virus-infected persons. J. Infect. Dis. **171:**837–844.
9. **Chakrabarti, L., P. Isola, M. C. Cumont, M. A. Claessens-Maire, M. Hurtrel, L. Montagnier, and B. Hurtrel.** 1994. Early stages of simian immunodeficiency virus infection in lymph nodes. Evidence for high viral load and successive populations of target cells. Am. J. Pathol. **144:**1226–1237.
10. **Chakrabarti, L., V. Baptiste, E. Khatissian, M. C. Cumont, A. M. Aubertin, L. Montagnier, and B. Hurtrel.** 1995. Limited viral spread and rapid immune response in lymph nodes of macaques inoculated with attenuated simian immunodeficiency virus. Virology **213:**535–548.
11. **Connor, R. I., D. C. Montefiori, J. M. Binley, J. P. Moore, S. Bonhoeffer, A. Gettie, E. A. Fenamore, K. E. Sheridan, D. D. Ho, P. J. Dailey, and P. A. Marx.** 1998. Temporal analyses of virus replication, immune responses, and efficacy in rhesus macaques immunized with a live, attenuated simian immunodeficiency virus vaccine J. Virol. **72:**7501–7509.
12. **Daniel, M. D., F. Kirchhoff, S. C. Czajak, P. K. Sehgal, and R. C. Desrosiers.** 1992. Protective effects of a live attenuated SIV vaccine with a deletion in the *nef* gene. Science **258:**1938–1941.
13. **Desrosiers, R. C.** 1999. Strategies used by human immunodeficiency virus that allow persistent viral replication. Nat. Med. **5:**723–725.
14. **Douek, D. C., J. M. Brenchley, M. R. Betts, D. R. Ambrozak, B. J. Hill, Y. Okamoto, J. P. Casazza, J. Kuruppu, K. Kunstman, S. Wolinsky, Z. Grossman, M. Dybul, A. Oxenius, D. A. Price, M. Connors, and R. A. Koup.** 2002. HIV preferentially infects HIV-specific $CD4^+$ T cells. Nature **417:**95–98.
15. **Du, Z., S. M. Lang, V. G. Sasseville, A. A. Lackner, P. O. Ilyinskii, M. D. Daniel, J. U. Jung, and R. C. Desrosiers.** 1995. Identification of a *nef* allele that causes lymphocyte activation and acute disease in macaque monkeys. Cell **82:**665–674.
16. **Dykhuizen, M., J. L. Mitchen, D. C. Montefiori, J. Thomson, L. Acker, H. Lardy, and C. D. Pauza.** 1998. Determinants of disease in the simian immunodeficiency virus-infected rhesus macaque: characterizing animals with low antibody responses and rapid progression. J. Gen. Virol. **79:**2461–2467.
17. **Fackler, O. T., and A. S. Baur.** 2002. Live and let die: Nef functions beyond HIV replication. Immunity **16:**493–497.
18. **Garcia, J. V., and A. D. Miller.** 1991. Serine phosphorylation-independent downregulation of cell-surface CD4 by nef. Nature **350:**508–511.
19. **Garside, P., E. Ingulli, R. R. Merica, J. G. Johnson, R. J. Noelle, and M. K. Jenkins.** 1998. Visualization of specific B and T lymphocyte interactions in the lymph node. Science **281:**96–99.
20. **Glushakova, S., J. C. Grivel, K. Suryanarayana, P. Meylan, J. D. Lifson, R. Desrosiers, and L. Margolis.** 1999. Nef enhances human immunodeficiency

virus replication and responsiveness to interleukin-2 in human lymphoid tissue ex vivo. J. Virol. **73:**3968–3974.
21. **Greenberg, M. E., A. J. Iafrate, and J. Skowronski.** 1998. The SH3 domain-binding surface and an acidic motif in HIV-1 Nef regulate trafficking of class I MHC complexes. EMBO J. **17:**2777–2789.
22. **Grossman, Z., M. Meier-Schellersheim, A. E. Sousa, R. M. Victorino, and W. E. Paul.** 2002. $CD4^+$ T-cell depletion in HIV infection: are we closer to understanding the cause? Nat. Med. **8:**319–323.
23. **Hu, J., M. B. Gardner, and C. J. Miller.** 2000. Simian immunodeficiency virus rapidly penetrates the cervicovaginal mucosa after intravaginal inoculation and infects intraepithelial dendritic cells. J. Virol. **74:**6087–6095.
24. **Johnson, R. P., J. D. Lifson, S. C. Czajak, K. S. Cole, K. H. Manson, R. Glickman, J. Yang, D. C. Montefiori, R. Montelaro, M. S. Wyand, and R. C. Desrosiers.** 1999. Highly attenuated vaccine strains of simian immunodeficiency virus protect against vaginal challenge: inverse relationship of degree of protection with level of attenuation. J. Virol. **73:**4952–4961.
25. **Johnson, R. P., and R. C. Desrosiers.** 1998. Protective immunity induced by live attenuated simian immunodeficiency virus. Curr. Opin. Immunol. **10:**436–443.
26. **Kestler, H. W., III, D. J. Ringler, K. Mori, D. L. Panicali, P. K. Sehgal, M. D. Daniel, and R. C. Desrosiers.** 1992. Importance of the *nef* gene for maintenance of high virus loads and for development of AIDS. Cell **65:**651–662.
27. **Kim, C. H., L. S. Rott, I. Clark-Lewis, D. J. Campbell, L. Wu, and E. C. Butcher.** 2001. Subspecialization of $CXCR5^+$ T cells: B helper activity is focused in a germinal center-localized subset of $CXCR5^+$ T cells. J. Exp. Med. **193:**1373–1381.
28. **Kirchhoff, F., T. C. Greenough, D. B. Brettler, J. L. Sullivan, and R. C. Desrosiers.** 1995. Absence of intact *nef* sequences in a long-term survivor with nonprogressive HIV-1 infection. N. Engl. J. Med. **332:**228–232.
29. **Lackner, A. A., P. Vogel, R. A. Ramos, J. D. Kluge, and M. Marthas.** 1994. Early events in tissues during infection with pathogenic (SIVmac239) and nonpathogenic (SIVmac1A11) molecular clones of simian immunodeficiency virus. Am. J. Pathol. **145:**428–439.
30. **Le Gall, S., L. Erdtmann, S. Benichou, C. Berlioz-Torrent, L. Liu, R. Benarous, J. M. Heard, and O. Schwartz.** 1998. Nef interacts with the mu subunit of clathrin adaptor complexes and reveals a cryptic sorting signal in MHC I molecules. Immunity **8:**483–495.
31. **Matano, T., M. Kano, T. Odawara, H. Nakamura, A. Takeda, K. Mori, T. Sata, and Y. Nagai.** 2000. A novel effective DNA vaccine strategy inducing safer confined replication of engineered vaccine virus mediated by foreign receptor. Vaccine **18:**3310–3318.
32. **Messmer, D., R. Ignatius, C. Santisteban, R. M. Steinman, and M. Pope.** 2000. The decreased replicative capacity of SIVmac239Δnef is manifest in cultures of immature dendritic cells and T cells. J. Virol. **74:**2406–2413.
33. **Miller, M. D., M. T. Warmerdam, I. Gaston, W. C. Greene, and M. B. Feinberg.** 1994. The human immunodeficiency virus-1 *nef* gene product: a positive factor for viral infection and replication in primary lymphocytes and macrophages. J. Exp. Med. **179:**101–113.
34. **Mori, K., Y. Yasutomi, S. Sawada, F. Villinger, K. Sugama, B. Rosenwith, J. L. Heeney, K. Uberla, S. Yamazaki, A. A. Ansari, and H. Rubsamen-Waigmann.** 2000. Suppression of acute viremia by short-term postexposure prophylaxis of simian/human immunodeficiency virus SHIV-RT-infected monkeys with a novel reverse transcriptase inhibitor (GW420867) allows for development of potent antiviral immune responses resulting in efficient containment of infection. J. Virol. **74:**5747–5753.
35. **Mori, K., Y. Yasutomi, S. Ohgimoto, T. Nakasone, S. Takamura, T. Shioda, and Y. Nagai.** 2001. Quintuple deglycosylation mutant of simian immunodeficiency virus SIVmac239 in rhesus macaques: robust primary replication, tightly contained chronic infection, and elicitation of potent immunity against the parental wild-type strain. J. Virol. **75:**4023–4028.
36. **Moritoyo, T., S. Izumo, H. Moritoyo, Y. Tanaka, Y. Kiyomatsu, M. Nagai, K. Usuku, M. Sorimachi, and M. Osame.** 1999. Detection of human T-lymphotropic virus type I p40tax protein in cerebrospinal fluid cells from patients with human T-lymphotropic virus type I-associated myelopathy/tropical spastic paraparesis. J. Neurovirol. **5:**241–248.
37. **Munch, J., N. Stolte, D. Fuchs, C. Stahl-Hennig, and F. Kirchhoff.** 2001. Efficient class I major histocompatibility complex down-regulation by simian immunodeficiency virus Nef is associated with a strong selective advantage in infected rhesus macaques. J. Virol. **75:**10532–10536.
38. **O'Connor, D. H., T. M. Allen, T. U. Vogel, P. Jing, I. P. DeSouza, E. Dodds, E. J. Dunphy, C. Melsaether, B. Mothe, H. Yamamoto, H. Horton, N. Wilson, A. L. Hughes, and D. I. Watkins.** 2002. Acute phase cytotoxic T lymphocyte escape is a hallmark of simian immunodeficiency virus infection. Nat. Med. **8:**493–499.
39. **Otani, I., K. Mori, T. Sata, K. Terao, K. Doi, H. Akari, and Y. Yoshikawa.** 1999. Accumulation of $MAC387^+$ macrophages in paracortical areas of lymph nodes in rhesus monkeys acutely infected with simian immunodeficiency virus. Microbes Infect. **1:**977–985.
40. **Patel, P. G., M. T. Yu Kimata, J. E. Biggins, J. M. Wilson, and J. T. Kimata.** 2002. Highly pathogenic simian immunodeficiency virus mne variants that emerge during the course of infection evolve enhanced infectivity and the ability to downregulate CD4 but not class I major histocompatibility complex antigens. J. Virol. **76:**6425–6434. (Erratum, **76:**8977.)
41. **Piguet, V., O. Schwartz, S. Le Gall, and D. Trono.** 1999. The downregulation of CD4 and MHC-I by primate lentiviruses: a paradigm for the modulation of cell surface receptors. Immunol. Rev. **168:**51–63.
42. **Pitcher, C. J., S. I. Hagen, J. M. Walker, R. Lum, B. L. Mitchell, V. C. Maino, M. K. Axthelm, and L. J. Picker.** 2002. Development and homeostasis of T cell memory in rhesus macaque. J. Immunol. **168:**29–43.
43. **Poudrier, J., X. Weng, D. G. Kay, G. Pare, E. L. Calvo, Z. Hanna, M. H. Kosco-Vilbois, and P. Jolicoeur.** 2001. The AIDS disease of CD4C/HIV transgenic mice shows impaired germinal centers and autoantibodies and develops in the absence of IFN-γ and IL-6. Immunity **15:**173–185.
44. **Reimann, K. A., K. Tenner-Racz, P. Racz, D. C. Montefiori, Y. Yasutomi, W. Lin, B. J. Ransil, and N. L. Letvin.** 1994. Immunopathogenic events in acute infection of rhesus monkeys with simian immunodeficiency virus of macaques. J. Virol. **68:**2362–2370.
45. **Rosenberg, E., M. Altfed. S. Poon, M. Phillips, B. Wilkes, R. Eldridge, G. Robbins, R. D'Aquila, P. Goulder, and B. Walker.** 2000. Immune control of HIV-1 following early treatment of acute infection. Nature **407:**523–526.
46. **Sallusto, F., D. Lenig, R. Forster, M. Lipp, and A. Lanzavecchia.** 1999. Two subsets of memory T lymphocytes with distinct homing potentials and effector functions. Nature **401:**708–712.
47. **Schnittman, S. M., H. C. Lane, J. Greenhouse, J. S. Justement, M. Baseler, and A. S. Fauci.** 1990. Preferential infection of $CD4^+$ memory cells by human immunodeficiency virus type 1: evidence for a role in the selective T-cell functional defects observed in infected individuals. Proc. Natl. Acad. Sci. USA **87:**6058–6062.
48. **Simmons, A., V. Aluvihare, and A. McMichael.** 2001. Nef triggers a transcriptional program in T cells imitating single-signal T cell activation and inducing HIV virulence mediators. Immunity **14:**763–777.
49. **Spina, C. A., H. E. Prince, and D. D. Richman.** 1997. Preferential replication of HIV-1 in the CD45RO memory cell subset of primary CD4 lymphocytes in vitro. J. Clin. Investig. **99:**1774–1785.
50. **Stahl-Hennig, C., R. M. Steinman, K. Tenner-Racz, M. Pope, N. Stolte, K. Matz-Rensing, G. Grobschupff, B. Raschdorff, G. Hunsmann, and P. Racz.** 1999. Rapid infection of oral mucosal-associated lymphoid tissue with simian immunodeficiency virus. Science **285:**1261–1265.
51. **Stahl-Hennig, C., R. M. Steinman, P. T. Haaft, K. Uberla, N. Stolte, S. Saeland, K. Tenner-Racz, and P. Racz.** 2002. The simian immunodeficiency virus Δ*nef* vaccine, after application to the tonsils of rhesus macaques, replicates primarily within $CD4^+$ T cells and elicits a local perforin-positive $CD8^+$ T-cell response. J. Virol. **76:**688–696.
52. **Swigut, T., N. Shohdy, and J. Skowronski.** 2001. Mechanism for down-regulation of CD28 by Nef. EMBO J. **20:**1593–1604.
53. **Tenner-Racz, K., H.-J. Stellbrink, J. van Lunzen, C. Schneider, J.-P. Jacobs, B. Raschdorff, G. Grosschupff, R. M. Steinman, and P. Racz.** 1998. The unenlarged lymph nodes of HIV-1 infected, asymptomatic patients with high CD4 T cell counts are sites for virus replication and CD4 T cell proliferation: the impact of active antiretroviral therapy. J. Exp. Med. **187:**949–959.
54. **Veazey, R. S., M. DeMaria, L. V. Chalifoux, D. E. Shvetz, D. R. Pauley, H. L. Knight, M. Rosenzweig, R. P. Johnson, R. C. Desrosiers, and A. A. Lackner.** 1998. Gastrointestinal tract as a major site of $CD4^+$ T cell depletion and viral replication in SIV infection. Science **280:**427–431.
55. **Veazey, R. S., I. C. Tham, K. G. Mansfield, M. A. DeMaria, A. E. Forand, D. E. Shvetz, L. V. Chalifoux, P. K. Sehgal, and A. A. Lackner.** 2000. Identifying the target cell in primary simian immunodeficiency virus (SIV) infection: highly activated memory $CD4^+$ T cells are rapidly eliminated in early SIV infection in vivo. J. Virol. **74:**57–64.
56. **Veazey, R. S., K. G. Mansfield, I. C. Tham, A. C. Carville, D. E. Shvetz, A. E. Forand, and A. A. Lackner.** 2000. Dynamics of CCR5 expression by $CD4^+$ T cells in lymphoid tissues during simian immunodeficiency virus infection. J. Virol. **74:**11001–11007.
57. **Zhang, Z., T. Schuler, M. Zupancic, S. Wietgrefe, K. A. Staskus, K. A. Reimann, T. A. Reinhart, M. Rogan, W. Cavert, C. J. Miller, R. S. Veazey, D. Notermans, S. Little, S. A. Danner, D. D. Richman, D. Havlir, J. Wong, H. L. Jordan, T. W. Schacker, P. Racz, K. Tenner-Racz, N. L. Letvin, S. Wolinsky, and A. T. Haase.** 1999. Sexual transmission and propagation of SIV and HIV in resting and activated $CD4^+$ T cells. Science **286:**1353–1357.